

PACS numbers: 41.75.Jv; 42.65.Re
DOI: 10.1070/QE2004v034n02ABEH002597

Laser acceleration of electrons in vacuum up to energies of $\sim 10^9$ eV

A. Bahari, V.D. Taranukhin

***Abstract*. A new mechanism of laser acceleration of charged particles is investigated in detail. Upon irradiation by tightly focused high-intensity ultrashort laser pulses, the acceleration of electrons travelling along the laser beam axis is determined by the longitudinal ponderomotive force and the longitudinal component of the electric field of the laser wave. It is found that the action of the longitudinal field on an electron may be unidirectional during many optical cycles, i.e., the phase slip effect is overcome. Lasers with currently highest possible parameters are shown to enable electron acceleration up to energies $\varepsilon \sim 1$ GeV, which is comparable to the energies attainable on 'large' accelerators of the SLAC type ($\varepsilon \sim 30 - 50$ GeV). Unlike the schemes considered in the literature, the acceleration in this case is insensitive to the initial field phase (the effect of electron bunching is absent), it is possible to accelerate slow (nonrelativistic) electrons, and the problem of accelerated electron extraction from the field does not exist.**

Keywords: *laser acceleration of electrons, ultrashort laser pulses, ponderomotive forces.*

1. Introduction

The modern progress of laser physics affords the generation of coherent laser radiation with an intensity $I \sim 10^{19} - 10^{21}$ W cm^{-2} [1, 2]. One of the main applications of this radiation is acceleration of charged particles. In a recently published series of papers [3 – 8], a numerical investigation was made of electron acceleration by a focused beam of high-intensity ($I \sim 10^{21} - 10^{22}$ W cm^{-2}) cw laser radiation in vacuum. The generation of electrons with an energy $\varepsilon \sim 1$ GeV in laboratory conditions was shown to be possible in principle.

However, the acceleration process considered in Refs [3 – 8] is largely random, because the relativistic electrons are considered to fly into the laser beam at an angle to the direction of its propagation. The electron 'capture' by the laser beam and its acceleration up to an energy $\varepsilon \sim 0.1 - 1$ GeV are possible only for specific entrance angles θ_0 and initial electron velocities V_0 as well as for a certain initial field phase φ_0. As a consequence, ε depends strongly on θ_0, V_0, and φ_0. Note that the highly accurate control of the parameters θ_0, V_0, and φ_0 is hardly possible. Furthermore, in the case of cw radiation there arises the problem of accelerated-electron extraction from the field. In Refs [3, 4], the use of a static magnetic field is proposed for the electron extraction, which complicates the experiment. In Refs [3 – 8], the specific acceleration mechanism was not elucidated.

In our work [9] we reported the possibility of electron acceleration by a short high-intensity laser pulse during the electron propagation along the axis of the laser beam ($\theta_0 = 0$). Numerical experiments showed that when a laser pulse 'collides' with an electron, which may have an arbitrary velocity along the wave vector $\boldsymbol{k}$, the acceleration is insensitive to the initial field phase φ_0 and the accelerated electron is automatically extracted from the field after the passage of the pulse. Therefore, in the 'longitudinal' scheme of electron – radiation interaction proposed in Ref. [9] it is possible to overcome the random character of acceleration, no prior electron acceleration to relativistic velocities is required, and the problem of accelerated electron extraction from the field is solved. Furthermore, in Ref. [9] we established the mechanism of laser-driven acceleration: it involves the combination of the longitudinal ponderomotive force, which arises due to the pulsed character of radiation, and the longitudinal component of the electric field of the laser wave, which emerges in the radiation focusing.

The mechanism brought to light owes its efficiency to the difference between the phase velocities of longitudinal and transverse electron motion, which takes place in focused laser beams. This difference makes it possible to overcome the effect of phase slip, which is the primary cause of limitation of the efficiency of charged particle acceleration by laser radiation (see, for instance, Ref. [10]).

Our work gives a detailed description of electron acceleration in the 'longitudinal' interaction scheme. We discuss the possibilities for improving the efficiency of this process due to optimisation of the parameters of laser radiation focusing, duration, and polarisation as well as due to the initial electron coordinates and velocities.

A. Bahari Department of Physics, M.V. Lomonosov Moscow State University, Vorob'evy Gory, 119992 Moscow, Russia;
V.D. Taranukhin International Teaching and Research Laser Center, M.V. Lomonosov Moscow State University, Vorob'evy Gory, 119992 Moscow, Russia

Received 15 July 2003
Kvantovaya Elektronika **34** (2) 129 – 134 (2004)
Translated by E.N. Ragozin

2. Action of a focused laser field on a relativistic electron

Consider the electron acceleration by a short pulse ($\tau \approx 20 - 100T$, where T is the time of the optical cycle) of tightly focused laser radiation: the radius of the laser beam waist is $w_0 \sim (5 - 50)\lambda$ ($\lambda \approx 1$ μm is the radiation wavelength). The electron motion is described by the relativistic equation for the electron momentum $\boldsymbol{p}$ (the effect of radiative deceleration is neglected) [11]

$$\frac{\mathrm{d}\boldsymbol{p}}{\mathrm{d}t} = \vec{\mathscr{E}} + \vec{\mathscr{M}}, \quad \vec{\mathscr{E}} = e\boldsymbol{E}, \quad \vec{\mathscr{M}} = \frac{e}{c}\,\boldsymbol{V} \times \boldsymbol{B},$$
$$\boldsymbol{p} = m\gamma\boldsymbol{V}, \ \gamma = \left(1 - \frac{V^2}{c^2}\right)^{-1/2}, \tag{1}$$

where $\boldsymbol{E}$ and $\boldsymbol{B}$ are the electric and magnetic fields of laser radiation; e and m are the electron charge and mass; t is the time; and c is the velocity of light. The focused laser radiation was defined in the parabolic approximation [12] correct to 2nd order in the small parameter $\xi = \lambda/2\pi w_0$. Unlike Refs [3–8], this accuracy is sufficient, because the electron motion in our case takes place near the laser beam axis: for any radiation intensities, the amplitude of electron oscillation does not exceed the radiation wavelength in the electron frame of reference (i.e., the wavelength calculated taking the Doppler effect into account). Dedicated calculations carried out with the inclusion of the terms of higher order in the parameter ξ (see below) showed that the inaccuracy of our approximation does not exceed 10 %. In this approximation, the components of the electric and magnetic radiation fields can be represented as

$$E_z = -\frac{E_0(\eta)}{kw^2}\exp\left(-\frac{x^2+y^2}{w^2}\right) \times [(x+y)\sin\varphi_\parallel + (x-y)\sin(\varphi_\parallel + \varphi_\mathrm{p})], \tag{2}$$

$$E_{x,y} = \frac{w_0 E_0(\eta)}{2w}\exp\left(-\frac{x^2+y^2}{w^2}\right) \times [\cos\varphi_\perp \pm \cos(\varphi_\perp + \varphi_\mathrm{p})], \tag{3}$$

$$B_z = -\frac{E_0(\eta)}{kw^2}\exp\left(-\frac{x^2+y^2}{w^2}\right) \times [-(x-y)\sin\varphi_\parallel + (x+y)\sin(\varphi_\parallel + \varphi_\mathrm{p})], \tag{4}$$

$$B_{x,y} = \mp\frac{w_0 E_0(\eta)}{2w}\exp\left(-\frac{x^2+y^2}{w^2}\right) \times [\cos\varphi_\perp \mp \cos(\varphi_\perp + \varphi_\mathrm{p})], \tag{5}$$

where E_0 is the field amplitude; $\varphi_\parallel = \varphi_\perp + \arctan(z/z_\mathrm{c})$, $\varphi_\perp = \varphi_0 + \eta + \arctan(z/z_\mathrm{c}) - z(x^2+y^2)/w^2 z_\mathrm{c}$ are the phases of the longitudinal and transverse field components; $w^2 = w_0^2[1 + (z/z_\mathrm{c})^2]$; $z_\mathrm{c} = kw_0^2/2$ is the diffraction length; $\eta = 2\pi t/T - kz$; φ_p is the parameter which defines the radiation polarisation (linear for $\varphi_\mathrm{p} = 0$ and circular for $\varphi_\mathrm{p} = \pi/2$); and $E_0(\eta)$ is the function which describes the pulse shape; coordinate axes are selected so that $\boldsymbol{z} \| \boldsymbol{k}$, $\boldsymbol{x}, \boldsymbol{y} \perp \boldsymbol{k}$, and the focus is at the point $z = 0$. Unlike Ref. [12], the components of the fields $\boldsymbol{E}$ and $\boldsymbol{B}$ as functions of the transverse coordinates x, y are explicitly defined.

Eqn (1) was solved, using expressions (2)–(5), by the 4th-order accurate Runge–Kutta technique for the electrons with different initial velocities $\boldsymbol{V}_0$ and positions z_0 relative to the focus as well as for laser pulses of different duration, polarisation and peak intensity I_0. The laser pulse shape (in the laboratory frame of reference) was defined as $E_0 \sim \exp[-(2t/\tau)^4]$. We considered pulses with a duration $\tau/T \approx (20 - 100) \gg 1$, which permits the use of a slowly varying field envelope approximation.

During numerical experiments, we controlled the total energy radiated by the electron ε_rad, which was calculated by a relativistic formula [11]. In all cases this energy was many orders of magnitude lower than the kinetic electron energy, which justifies the neglect of radiative deceleration in Eqn (1). Note that the negligibility of radiation (and hence the negligibility of radiative deceleration) is favoured by the fact that the electron in our scheme is accelerated to a large measure by the longitudinal electric field. In this case, the relativistic expression for ε_rad is in essence reduced to the nonrelativistic one.

To interpret the results, it is instructive to see how the fields (2)–(5) change in going over to the electron frame of reference. In this frame of reference, the coordinates x, y, which enter in expressions (2)–(5), are time-dependent (or dependent on the current electron coordinate z), and the difference of the phases $\varphi_\parallel$ and $\varphi_\perp$, which simultaneously enter in the expressions for the longitudinal fields, can be of great importance.

First we consider the case of linearly polarised laser radiation. Fig. 1 shows the dependence of the longitudinal component of the laser wave electric field, which acts on the electron, on the current coordinate z. One can see that the longitudinal field E_z (or the force $\mathscr{E}_z$) oscillates. However, these oscillations change in character as the electron passes through the radiation focal region. In front of the focus, the amplitude of $\mathscr{E}_z$-force oscillations in the negative half-cycle is greater than in the positive one, resulting integrally in electron deceleration. In the focal region, the action of longitudinal electric field is, on the average, zero (the oscillations are symmetric). Upon electron passage through the focus, the $\mathscr{E}_z$-force amplitude in the positive half-cycle is

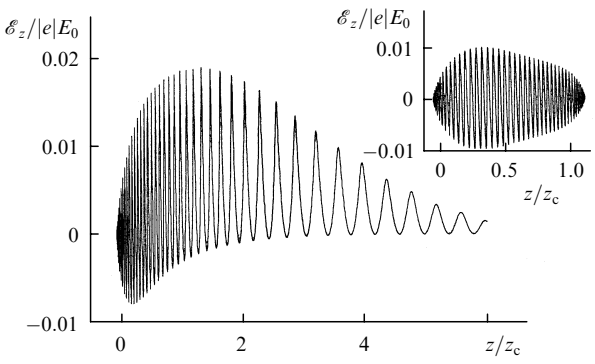

Figure 1. Variation in the longitudinal electric field, which acts on an electron during its interaction with linearly polarised pulsed radiation with $\tau = 20T$, a peak intensity $I_0 = 5 \times 10^{19}$ W cm^{-2}, and $w_0 = 5\lambda$ ($\boldsymbol{V}_0 = 0$, $z_0 = -5\lambda$, $x_0 = y_0 = 0$). The inset shows the same variation in the case when the phases $\varphi_\parallel$ and $\varphi_\perp$ are artificially equalised ($\varphi_\parallel = \varphi_\perp$).

greater than in the negative one. Moreover, the oscillations become practically unipolar at distances of the order of several diffraction lengths behind the focus, as will be apparent from Fig. 1. Despite the phase slip effect, this character of oscillations of the field E_z ensures efficient electron acceleration. It is only required that the electron should have a sufficiently high velocity and have time to move to the E_z field 'unipolarity' region from the focal region (where the radiation intensity is highest and where the electron–laser pulse interaction should begin) prior to the end of the laser pulse.

To demonstrate the effect of the difference between the phases $\varphi_\parallel$ and $\varphi_\perp$ we analysed the hypothetical case whereby $\varphi_\parallel = \varphi_\perp$. It turned out that the field E_z oscillates symmetrically throughout the period of interaction with the electron (see the inset in Fig. 1) and electron acceleration drastically decreases. Therefore, the significant effect of longitudinal laser field on electron acceleration is explained by the fact that the action of this field is determined by two factors, which oscillate with different phases: $\varphi_\parallel$ and $\varphi_\perp$. When the laser radiation is polarised along the x axis, from expressions (2) and (3) one can obtain the following estimate:

$$E_z \sim x(t_\mathrm{i}) \sin\varphi_\parallel, \quad x(t_\mathrm{i}) \sim \cos\varphi_\perp, \tag{6}$$

where t_i is the electron–radiation interaction time. From the phase relation

$$\varphi_\parallel - \varphi_\perp = \arctan\frac{z}{z_\mathrm{c}} \tag{7}$$

it follows that $\varphi_\parallel = \varphi_\perp$ and $E_z \sim \sin(2\varphi_\parallel)$ near the focus ($z = 0$), i.e., that the longitudinal field oscillates symmetrically. However, when the electron finds itself in the region behind the focus, the phase difference $(\varphi_\parallel - \varphi_\perp)$ tends to $\pi/2$, and $E_z \sim \sin^2(\varphi_\parallel)$, i.e., the oscillations of the longitudinal field become unipolar. We note that the transverse drift of the electron (except for the oscillatory component of its transverse motion) leads to bipolar, though asymmetric, oscillations of the field E_z. In our numerical experiments this drift was, as a rule, absent or was insignificant. As can be seen from Fig. 1, the field oscillations (for sufficiently great z) are practically unipolar.

For circularly polarised radiation, the longitudinal field E_z (in the moving electron frame of reference) varies smoothly without oscillations. However, the character of this variation remains as before. In front of the focus, the force $\mathscr{E}_z$ which acts on the electron is negative, $\mathscr{E}_z = 0$ in the focal region, and $\mathscr{E}_z > 0$ behind the focus.

The force $\mathscr{M}_z$ also varies smoothly in the case of circular polarisation and oscillates for a linear polarisation. In the latter case, its value averaged over the fast oscillations is the longitudinal ponderomotive force. We note that both the force $\mathscr{M}_z$ (for a circular polarisation) and its average value (for a linear polarisation) are proportional to the derivative $\partial I/\partial t$, i.e., to the longitudinal spatial gradient of the intensity of the laser pulse. In the subsequent discussion we apply the term 'longitudinal ponderomotive force' both to the force $\mathscr{M}_z$ (for circularly polarised radiation) and to its average value (for a linear polarisation).

The above features of the action of the longitudinal electric field on the electron moving along the laser beam axis gives rise to the possibility of efficient electron acceleration. This is explained by the fact that when the initial position of the electron z_0 is properly selected, the adverse action of the phase slip effect is overcome. As noted above, this effect is the principal limiting factor when other schemes of laser-driven charged particle acceleration are employed. The effect of unipolarity of the longitudinal electric field is supposedly responsible (at least in part) also for the electron acceleration in the numerical experiments carried out in Refs [3–8]. We are reminded that the physical interpretation of the results obtained in these papers is missing.

3. Results of numerical experiments on electron acceleration by a short laser pulse

Fig. 2 shows the results of numerical experiments on electron acceleration in the longitudinal scheme for strongly focused laser radiation of different polarisation. One can see that the energy acquired by the electron is highest when use is made of circularly polarised radiation. For a linear polarisation we performed calculations for the fields $\boldsymbol{E}$ and $\boldsymbol{B}$ in the parabolic approximation correct to terms $\sim \xi$ as well as with a higher accuracy ($\sim \xi^3$).

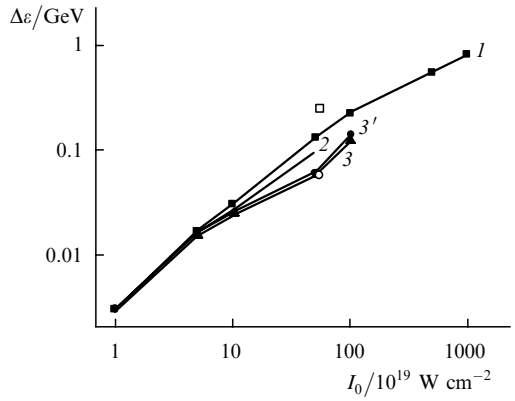

Figure 2. Dependence of the energy $\Delta\varepsilon$ acquired by an electron on the peak intensity I_0 for circularly ($\varphi_\mathrm{p} = \pi/2$) (*1*), elliptically ($\varphi_\mathrm{p} = \pi/4$) (*2*), and linearly ($\varphi_\mathrm{p} = 0$) (*3*, *3′*) polarised radiation for $\tau = 20T$, $w_0 = 10\lambda$, $V_{0z}/c = 0.9$, $z_0 = z_\mathrm{opt}$, and $x_0 = y_0 = 0$. For linearly polarised radiation, use was made of the fields calculated to the terms $\sim\xi$ (*3*) and $\sim\xi^3$ (*3′*). Also given are the results of calculations for the conditions of the numerical experiment of Ref. [5] for linearly polarised fields calculated to the terms $\sim\xi$ (○) and $\sim\xi^3$ (□) for inclined electron entry into the laser beam ($\theta_0 = 6^\circ$).

A comparison of the curves (*3*) and (*3′*) in Fig. 2 shows that the error of the approximation used in our work ($\sim \xi$) does not exceed 10 % in comparison with the case when the $\sim \xi^3$ approximation was drawn on. We note that in Ref. [5], which considered the electron transit at an angle to the laser beam axis, this error was equal to 75 %. This testifies to a higher sensitivity of the model to the accuracy of description of the focused radiation in the electron motion far from the laser beam axis.

To verify this fact we carried out the calculations of acceleration of the electron also for its propagation at an angle to the laser beam axis (analogously to the numerical experiments of Refs [3–8]). As Fig. 2 suggests, the error due to the use of a simpler model of the focused field ($\sim \xi$) in this case amounts to 75 %, which coincides with the result

obtained in Refs [3–5]. Therefore, in the longitudinal acceleration scheme, which was proposed in Ref. [9], the parabolic approximation, correct to the terms of the 2nd order in the small parameter $\xi = \lambda/2\pi w_0$, is quite sufficient and permits performing a wide range of numerical calculations.

Fig. 3 shows the longitudinal electron velocity V_z, the intensity of laser radiation I, as well as the longitudinal electric ($\mathscr{E}_z$) and 'magnetic' ($\mathscr{M}_z$) forces (in the electron frame of reference) as functions of longitudinal coordinate z for circularly polarised radiation. One can see that the force $\mathscr{M}_z$ acts in qualitatively the same manner as in the plane wave: $\mathscr{M}_z$ accelerates the electron at the pulse front, but decelerates it at the trailing edge of the pulse. In the absence of radiation focusing, this has the effect that the electron energy ε remains invariable upon cessation of the pulse: $\Delta\varepsilon = 0$ [13]. The action of focusing manifests itself in two ways.

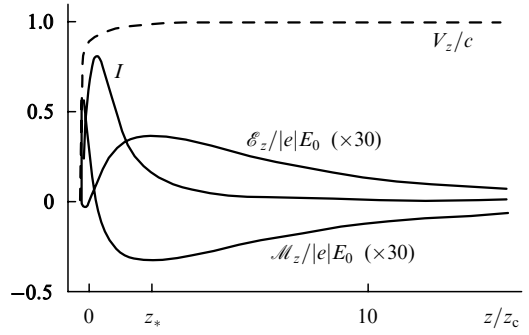

Figure 3. Dependences of the normalised longitudinal electron velocity V_z as well as of laser radiation intensity I, longitudinal electric ($\mathscr{E}_z$) and 'magnetic' ($\mathscr{M}_z$) forces (in the electron frame of reference) on the longitudinal z coordinate for circularly polarised radiation with a peak intensity $I_0 = 10^{20}$ W cm^{-2} for $\tau = 20T$, $w_0 = 5\lambda$ ($V_0 = 0$, $z_0 = -20\lambda$, $x_0 = y_0 = 0$); z_* is the characteristic point corresponding to the peak of the field E_z.

First, the integral action of the force $\mathscr{M}_z$ is nonzero. Numerical experiments revealed that $\int_{z_0}^{\infty} \mathscr{M}_z \mathrm{d}z < 0$ for the optimal selection of the initial electron coordinate z_0. This is due to the increase in radiation pulse duration (in the electron frame of reference) and different character of the radiation intensity variation at the front and the trailing edge of the laser pulse in different z regions. For instance, the intensity at the leading edge of the pulse in front of the focus rises faster (and decreases slower at the trailing edge) than in the plane wave. Accordingly, behind the focus the rate of the intensity decrease at the trailing edge of the pulse is higher and the intensity growth rate at its front is lower than in the plane wave.

Second, the radiation focusing leads to the emergence of longitudinal electric field E_z, which exerts a substantial effect on electron acceleration. In accordance with the analysis performed in Section 2, the field E_z first decelerates the electron (in the region in front of the focus) and then (for $z > 0$) compensates for the decelerating action of the force $\mathscr{M}_z$. For a strong focusing and a relatively high radiation intensity this compensation may be complete. The latter is confirmed by the dependence of the ratio $|\mathscr{E}_z/\mathscr{M}_z|$ at the characteristic point z_* (see Fig. 3), which corresponds to the peak of the field E_z, on the peak intensity of the laser pulse

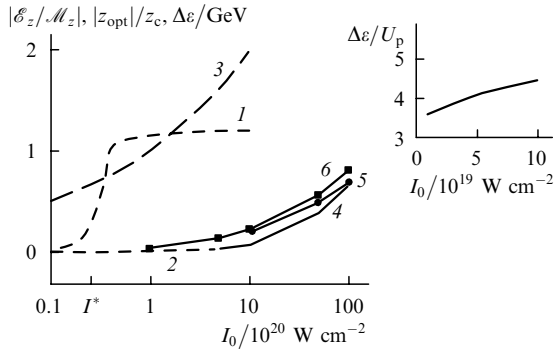

Figure 4. Dependences of the ratio $|\mathscr{E}_z/\mathscr{M}_z|$ at the characteristic point z_* (see Fig. 3) on the intensity of laser radiation I_0 for the parameter values specified in Fig. 3 (*1*), the same for $\varphi_\parallel = \varphi_\perp$ (*2*); plotted for circularly polarised radiation ($\tau = 20T$, $w_0 = 10\lambda$, $V_{0x} = V_{0y} = 0$, $x_0 = y_0 = 0$) are the I_0-dependences of the optimal initial electron coordinate z_{opt} for $V_{0z} = 0.9c$ (3) and the electron energy $\Delta\varepsilon$ for the initial velocities $V_{0z} = 0$ (*4*), 0.5 (*5*), and 0.9 (*6*). The inset shows the I_0-dependence of $\Delta\varepsilon$ for circularly polarised radiation and the optimal focusing $w_0 = w_{opt}$ ($\tau = 20T$, $z_0 = z_{opt}$, $x_0 = y_0 = 0$, $V_{0x} = V_{0y} = 0$, $V_{0z} = 0.9c$).

I_0. Referring to Fig. 4, the ratio $|\mathscr{E}_z/\mathscr{M}_z|_{z*} \geqslant 1$ when the intensity is high enough ($I_0 > I^*$), so that all the energy acquired by the electron due to the longitudinal ponderomotive force $\mathscr{M}_z$ is retained (or even increases) upon cessation of the laser pulse.

This dependence is explained as follows: as the intensity I_0 rises, the electron velocity increases (initially, due to the longitudinal ponderomotive force). In this case, the longitudinal field E_z remains invariable in the frame of reference moving with a velocity V_z (in accordance with the Lorentz transformation), the force $\mathscr{M}_z \sim \partial(E_0/\omega)^2/\partial z$ [14] decreases, since the ratio E_0/ω is a relativistic invariant (in the plane-wave approximation), and the characteristic spatial scale Δz of the laser pulse for the co-moving electron increases. This character of variation of the forces $\mathscr{E}_z$ and $\mathscr{M}_z$ results in an even greater electron acceleration, and the $|\mathscr{E}_z/\mathscr{M}_z|_{z_*}$ ratio growth becomes avalanche-like (Fig. 4). We note once again that the intensity of laser radiation should be high enough ($I_0 > I^*$) to 'trigger' this positive feedback. At the same time, when the phases are artificially equalised ($\varphi_\parallel = \varphi_\perp$) the ratio $|\mathscr{E}_z/\mathscr{M}_z|_{z_*} \ll 1$ [curve (*2*) in Fig. 4] and there occurs no electron acceleration.

Therefore, the following scenario of energy gain by the electron is realised in the longitudinal acceleration scheme. Due to the action of the longitudinal ponderomotive force $\mathscr{M}_z$ at the front of the laser pulse, a slow or even an immobile electron is accelerated to a relativistic velocity, its initial position in front of the focus ($z_0 < 0$) proving to be optimal for maximising the electron energy gain. In the early stage, the longitudinal electric field therefore decelerates the electron. When the electron finds itself at the trailing edge of the pulse, the force $\mathscr{M}_z$ begins to decelerate it. However, for the optimal selection of the initial parameters the electron is already behind the focus, and the longitudinal electric field compensates for the deceleration completely. It is significant that the final electron energy is independent of the initial field phase φ_0 with this acceleration mechanism, because in the course of acceleration the electron experiences the phase slip during all optical cycles of the laser pulse. In this case, the effect of bunching does not occur – the input electron beam does not split into spatially separated bunches.

Moreover, the final electron energy has only a weak dependence also on its initial velocity V_0 (see Fig. 4). The last circumstance is explained by the fact that the required electron acceleration is effected by the laser pulse itself (other schemes of laser-driven acceleration [3–8] necessitate prior electron acceleration to relativistic velocities).

For a linear radiation polarisation, the forces $\mathscr{E}_z$ and $\mathscr{M}_z$ oscillate in time. However, the electron acceleration scenario remains, in the mean, the same as for a circular polarisation. We only note that the final electron energy is lower by 20 % in this case (see Fig. 2).

This laser-driven acceleration mechanism has not been discussed so far. It becomes significant only with a strong focusing and the use of ultrashort high-intensity radiation pulses ($I_0 > I^*$). Note that the intensity I^* (whereby $|\mathscr{E}_z| \approx |\mathscr{M}_z|$ on the tail of the laser pulse) decreases as the initial electron velocity V_0 increases. There is one more point in favour of the fact that the acceleration mechanism is not purely 'ponderomotive' in our scheme: for certain parameters of laser radiation and initial parameters of the electron its final energy is substantially greater than the ponderomotive radiation potential U_p (see the inset in Fig. 4). In this case, the focusing (the emergence of longitudinal electric field E_z) is of crucial importance in electron acceleration, which is proved by special calculations in which the field E_z was artificially set equal to zero. In these calculations (for any radiation intensity I_0), the electron energy remains unchanged after the passage of the laser pulse ($\Delta\varepsilon = 0$).

4. Optimisation of the initial parameters

Attaining ultimate energies calls for the optimisation of both the initial radiation parameters and the initial electron parameters. Since we consider the electron acceleration in vacuum, there are no limitations on the radiation intensity. In view of the progress of laser technology, at present one can figure on employing laser sources with a peak intensity I_0 up to $10^{20} - 10^{22}$ W cm^{-2} [1, 2]. As already noted, it is better to use circularly polarised radiation. In this case, there exists an optimal laser pulse duration (Fig. 5). A shorter pulse provides a stronger longitudinal ponderomotive force (for a fixed intensity I_0) and a longer pulse provides a deeper electron advance into the region of 'unipolar' field E_z.

The effect of pulse rise time τ_1 on electron acceleration is shown by [curve (*3*)] in Fig. 5. Lengthening the pulse fall time τ_2 for a fixed pulse rise time leads to a certain increase in final electron energy. Note, however, that employing pulses with a significantly longer fall time is disadvantageous for a strong focusing, because the radiation intensity drops sharply in the region behind the focus (even for an infinitely long pulse).

The effect of varying the initial electron velocity is shown in Fig. 4: the energy $\Delta\varepsilon$ rises with V_{0z}, but this rise is not large, because the electron is mostly accelerated by the laser pulse itself (by the longitudinal ponderomotive force). The dependence of acceleration on the initial electron coordinate z_0 is more complicated.

Calculations showed that there exists an optimal initial coordinate z_{opt} (distance to the focus), whereby the energy $\Delta\varepsilon$ acquired by the electron is highest. This takes place in the case that the electron spends, during the laser pulse, rather much time in the focal region ($z \approx 0$), where the radiation intensity is highest, and at the same time enters the 'unipolarity' region ($z \sim z_c$), where the action of longitudinal electric field is most efficient. With increase in initial electron velocity V_{0z} and peak radiation intensity I_0, the length z_{opt} increases (see Fig. 4).

There also exists an optimal radius of focusing w_{opt} (Fig. 6). The nonmonotone dependence $\Delta\varepsilon(w_0)$ follows from expressions (2) and (3), which define the explicit dependence of the field E_z on w_0 and the dependence of transverse electron coordinates ($x, y \sim w_0/w$) on w_0. On the whole we have

$$E_z \sim w_0^{-2}\left[1 + \left(\frac{z}{z_c}\right)^2\right]^{-3/2}, \qquad (8)$$

where account should be taken of the dependence of the effective electron mass on w_0 and also the fact that $z_c \sim w_0^2$. The non-monotonicity of the dependence of electron energy on the radius of focusing becomes clear when it is considered that the field E_z should be strong enough not only in the focal region, but in the 'unipolarity' domain behind the focus. Note that the optimal radius of focusing w_{opt} increases with peak intensity I_0 (see the inset in Fig. 6).

For presently ultimate intensities I_0, the optimal focusing may prove to be unattainable owing to the limitations on the output power of modern laser sources ($P \lesssim 10$ PW). How-

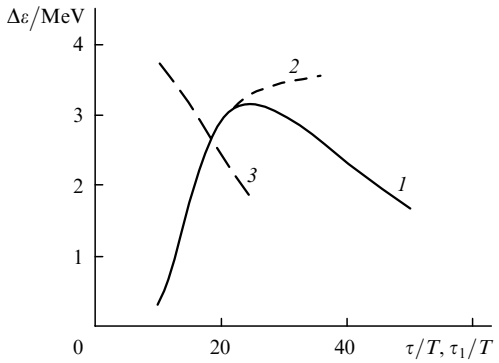

Figure 5. Dependences of the electron energy $\Delta\varepsilon$ on the duration τ of a circularly polarised laser pulse for $I_0 = 10^{19}$ W cm^{-2} ($V_{0z} = 0.9c$, $V_{0x} = V_{0y} = 0$, $w_0 = 10\lambda$, $z_0 = -157\lambda$, $x_0 = y_0 = 0$) (*1*), for a fixed pulse rise time ($\tau_1 = 10T$) and a varied fall time τ_2 ($\tau_1 \leqslant \tau_2 \leqslant \infty$) (*2*), and also the dependence $\Delta\varepsilon(\tau_1/T)$ for $\tau_2 = \infty$ (*3*).

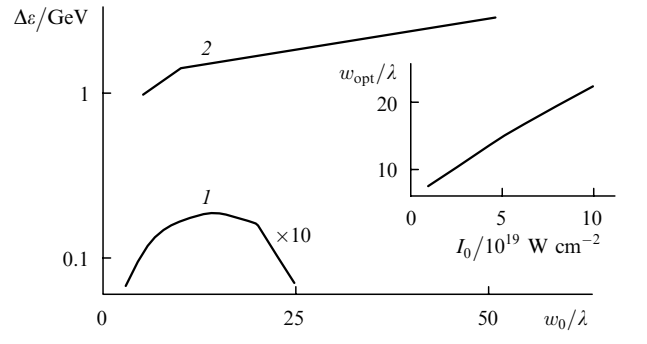

Figure 6. Dependence of the electron energy $\Delta\varepsilon$ on w_0 for circularly polarised radiation with $I_0 = 5 \times 10^{19}$ (*1*) and 10^{22} W cm^{-2} (*2*) for $\tau = 20T$, $V_{0z} = 0.9c$, $V_{0x} = V_{0y} = 0$, $z_0 = z_{opt}$, and $x_0 = y_0 = 0$. The inset shows the optimal radius w_{opt} against peak intensity I_0 for the same parameters.

ever, considering the prospects of laser technology development we performed numerical calculations also for the radiation with $I_0 = 10^{22}$ W cm^{-2}, $w_0 = 50\lambda$ [curve (*2*) in Fig. 6], which revealed the feasibility of electron acceleration up to energies exceeding several gigaelectronvolts. For a presently more realistic situation ($I_0 = 10^{22}$ W cm^{-2}, $w_0 = 10\lambda$), numerical experiments show the feasibility of attaining an energy $\varepsilon \sim 1$ GeV (Fig. 2), which is comparable to energies obtained on 'large' accelerators like that as SLAC.

In the end we consider the possibility of accelerating electrons whose initial velocity is not exactly coincident with the direction of laser radiation propagation ($\theta_0 \neq 0$). Fig. 7 shows the energy $\Delta\varepsilon$ acquired by the electron as a function of angle θ_0. The energy $\Delta\varepsilon$ decreases with increasing θ_0, which is due to the escape of the electron from the laser beam (in the transverse direction) prior to the acquisition of maximum energy. In this case, the characteristic angular scatter whereby $\Delta\varepsilon$ is insignificantly changed is $\delta\theta_0 \sim 5 - 10^\circ$, which is much greater than in the scheme with a 'side' electron entry into the laser beam [3–8]. For the parameters specified in Fig. 7, the $\Delta\varepsilon(\theta_0)$ dependence exhibits a maximum located at very small, though nonzero, angles θ_0. This maximum is interpreted as follows: the electron can gain an additional energy at exit from the beam in the transverse direction (owing to the transverse ponderomotive force) without significant loss in the energy of longitudinal motion. Optimisation of the θ_0 angle for the radiation with a peak intensity $I_0 = 10^{20}$ W cm^{-2} enables the maximum electron energy to be increased by about 40 %. At the same time, we revealed no additional peak in the $\Delta\varepsilon(\theta_0)$ distribution for the radiation with $I_0 = 10^{22}$ W cm^{-2}.

In conclusion we consider the possibility of electron beam acceleration in the longitudinal scheme (when the initial coordinates of the electrons correspond to their different positions relative to the laser beam axis). Fig. 8 shows the energy and exit-angle accelerated-electron distributions in this case. One can see that there occurs no significant departure $\Delta\theta$ of electron trajectories from the laser beam axis ($\Delta\theta < 0.1\pi$).

5. Conclusions

We have discovered and interpreted a new mechanism of laser acceleration of electrons, which is efficient only for short high-intensity laser pulses. It relies on the action of both the transverse and longitudinal fields of focused laser radiation. In this case, a significant part in the acceleration is played by the difference in the phase velocities of the transverse and longitudinal electron motion. In the proposed scheme, the random nature of acceleration is overcome, no prior electron acceleration to relativistic velocities is required, and the problem of accelerated-electron extraction from the field is solved. We have shown that this mechanism can provide the acceleration of electrons to energies $\varepsilon \gtrsim 1$ GeV in laser laboratories, which is comparable to the energies attainable on 'large' accelerators like that at SLAC.

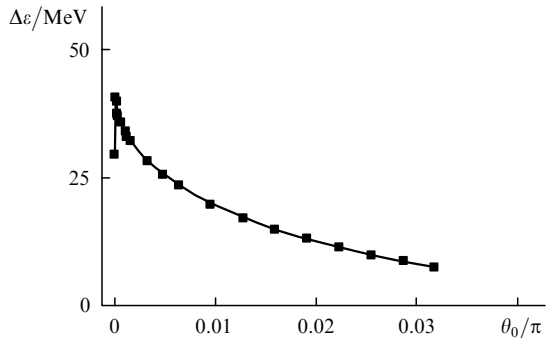

Figure 7. Dependence of the electron energy $\Delta\varepsilon$ on the angle θ_0 between the direction of propagation of circularly polarised laser radiation and the initial electron velocity for $I_0 = 10^{20}$ W cm^{-2}, $\tau = 20T$, $V_{0z} = 0.9c$, $z_0 = -0.1z_c$, $x_0 = y_0 = 0$, and $w_0 = 30\lambda$.

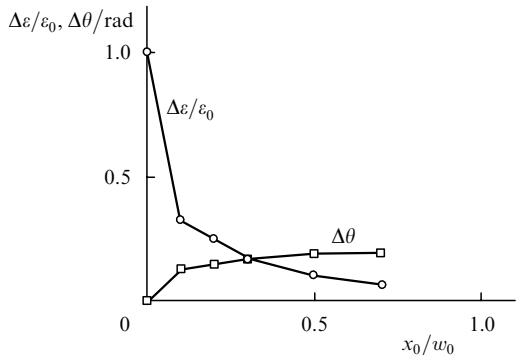

Figure 8. Angular departure of the electron from the laser beam axis $\Delta\theta$ and electron energy $\Delta\varepsilon$ as functions of its initial transverse coordinate x_0 for circularly polarised radiation with $I_0 = 10^{20}$ W cm^{-2}, $\tau = 20T$, $w_0 = 10\lambda$ ($V_{0z} = 0.9c$, $V_{0x} = V_{0y} = 0$, $z_0 = z_{\text{opt}}$); ε_0 is the energy corresponding to the $x_0 = 0$ coordinate.

References

1. Perry M.D., Pennington D., Stuart B.C., et al. *Opt. Lett.*, **24**, 160 (1999).
2. Tajima T., Mourou G., in *Superstrong fields in plasmas*. Ed. by M. Lontano, G. Mourou, O. Svelto, T. Tajima. (New York: Melville, 2002) Vol. 611, pp 423–436.
3. Salamin Y.I., Mocken G.R., Keitel C.H. *Phys. Rev. E*, **67**, 016501 (2003).
4. Salamin Y.I., Mocken G.R., Keitel C.H. *Phys. Rev. ST Accel. Beams*, **5**, 101301 (2002).
5. Salamin Y.I., Keitel C.H. *Phys. Rev Lett.*, **88**, 095005 (2002).
6. Kong Q., Ho Y.K., Wang J.X., et al. *Phys. Rev. E*, **61**, 1981 (2000).
7. Wang P.X., Ho Y.K., Yuan X.Q., et al. *Appl. Phys. Lett.*, **78**, 2253 (2001).
8. Wang J.X., Ho Y.K., Kong Q., et al. *Phys. Rev. E*, **58**, 6575 (1998).
9. Bahari A., Taranukhin V.D. *Kvantovaya Elektron.*, **33**, 563 (2003) [*Quantum Electron.*, **33**, 563 (2003)].
10. Scully M.O., Zubairy M.S. *Phys. Rev. A*, **44**, 2656 (1991).
11. Landau L.D., Lifshits E.M. *The Classical Theory of Fields* (Oxford: Pergamon Press, 1975).
12. Davis L.W. *Phys. Rev. A*, **19**, 1177 (1979).
13. Sarachik E.S., Shappert G.T. *Phys. Rev. D*, **1**, 2738 (1970).
14. Taranukhin V.D. *Zh. Eksp. Teor. Fiz.*, **117**, 511 (2000).